國立清華大學生命科學院

分子醫學研究所

碩士論文

發育中兔子視網膜內 Alpha 節細胞時空感受域的成熟過程

Spatiotemporal Receptive Fields of Alpha Ganglion Cells in the Developing Rabbit Retina

指導教授：焦傳金 博士 (Dr. Chuan-Chin Chiao)

研 究 生：李珣 (Hsun Li)

學　　號：g9580522

中華民國九十八年六月

摘　要

先前的研究指出，約在兔子睜開眼睛的時期，兔子視網膜節細胞就能對光刺激產生反應，在這個發育階段，視網膜節細胞已展現一些生理特性（例如感受域的同中心結抗性）。然而在兔子開眼後，視網膜節細胞會持續經歷細胞形態改變，以及感受域的微調整。因此本研究主要在檢視發育過程中，視網膜節細胞的生理功能和形態特性，並嘗試研究兩者之間的關係。從分屬三個不同發育時期的紐西蘭白兔取得實驗所用的視網膜後，利用白噪音視覺刺激引發視網膜節細胞反應，由胞外記錄的方式量測，經分析可得到觸發神經衝動的平均刺激，以代表視網膜節細胞的時空感受域。其後利用染劑注射視網膜節細胞，得到細胞形態來和平均刺激的空間結構互相比較。結果顯示，平均刺激的時間特性，會漸進地成熟；在出生後約兩週到三週、及三週後，alpha 視網膜節細胞所需對光刺激的整合時間，會逐漸減少。此外，對於光刺激產生穩定反應的能力，也會在出生後三週左右發生調整。然而，平均刺激的空間結構，和細胞樹突密度的關連程度不高，發育過程中也無明顯改變。所以本研究的結果顯示，視網膜節細胞的一些生理功能，在動物開眼後仍會繼續發育，但和細胞形態的微調無關。既然已知哺乳類視網膜中的緞帶突觸，會在相近的發育階段趨於成熟，因此，這些視網膜生理功能的改變，很可能是和緞帶突觸的發育有關。

關鍵字： 視網膜節細胞，感受域，發育

Abstract

Previous studies showed that rabbit retinal ganglion cells (RGCs) are responsive to light stimuli at around eye opening (postnatal day P10-11), and some of their physiological features (e.g., concentric receptive field antagonism) are also present at this developmental stage. However, active morphological remodeling of RGCs and fine tuning of their receptive fields are still continuing to proceed after eye opening. Thus, I investigated the physiological and morphological properties of RGCs throughout development, and attempted to examine the correlation between these two aspects. Ganglion cells from isolated retinas of New Zealand White rabbits were studied at three postnatal stages. The spatiotemporal receptive field properties of the alpha RGCs were characterized using the white noise stimuli, and the corresponding spike triggered average (STA) results were analyzed. After extracellular recording, the alpha cells were injected with dye to allow a direct comparison between the morphological pattern and their spatial STA profiles. The results showed that the maturation of STA time course is a gradual process during the development, that is, alpha RGCs gradually decrease their stimulus integration time from P10-14 to P20-23 then to adult. In addition, the robustness of the alpha RGC response to light stimulation is also developmentally modulated, and its main effect occurs before P20. Furthermore, moderate correlations between spatial STA

profiles and dendritic densities of both ON and OFF alpha RGCs do not change throughout development. Taken together, these results support that some functional properties of RGCs are indeed still developing even after eye-opening, and reveal that the morphological refinement of RGCs is independent of their physiological maturation. Given the fact that the ribbon synapses also develop at the same stages in the mammalian retina and their involvement in regulating response dynamics, it is likely that the changes of some functional properties of RGCs depend on the development of ribbon synapse.

Key words: RGC, receptive field, development

誌謝

這本論文終於完成了。想起這幾年在身邊支持我的每一個人，只有滿滿的感謝。

最要感謝的是，焦傳金老師，從指導我研究的方向，教導我解決實驗和程式上的問題，包容我不夠積極的態度，到修改我的論文，和給予其他許多幫助；而老師對科學的熱情和態度，也始終是我最佩服和還需要學習的。感謝張兗君老師和楊恩誠老師，擔任我的口試委員，以及在論文上給予的寶貴建議。

感謝實驗室的每一位成員，我的碩士學業能順利完成，很大一部份是因為你們的關係，讓我覺得自己真的很幸運，能在這個實驗室和你們一起學習、生活。芸潔學姊，很佩服你總是那麼有辦法，也謝謝你給過的幫忙；雅婷學姊，總是因為有你的鼓勵就覺得有了動力，更別說你在實驗上對我的鼎力相助；懿欣學姊，也是我多年的室友，忍受我混亂的作息，還在實驗室提供神奇料理；宏雅，和你一起當科宅的日子，日後回想起來也會科科地笑吧。還有雖然一起在實驗室的時間比較短，但也很感謝的學長姊，慧儒，總是說出讓我折服的道理和建議；紹瑋，幫助過我解決電腦和實驗方面的問題；沐霖，在我剛來實驗室時教我做實驗；家豪，是厲害又有趣的學長。讓實驗室充滿更多活力和歡樂的學弟妹們，芠軒、冠陵、怡廷、詩蓉、尹芃、品蒨、志揚和彥宏，也謝謝你們。至於雅茜，個性好又認真的你，我真的不能再感謝你更多，從一開始悉心地教我做實驗，每次報告、做海報甚至寫論文和準備口試時，給過我的各種幫忙和意見，你才是這論文的第二大推手。謝謝你們，讓我這幾年的生活豐富充實，無法回報什麼，只能真心祝福大家在研究上，和各方面

都能順利或成功吧。

感謝爸爸媽媽，一直以來給我的精神上的支持，還有經濟上的支持，讓我很自由地做自己想做的事，感謝幽默又不俗的妹妹，分享彼此的生活，偶爾也幫我補充一些人文素養。感謝曾信華學長在實驗技術上給予幫忙。也感謝所有給過我建議、鼓勵的師長，同學朋友，和學長姊學弟妹們。

最後還要謝謝因為這論文犧牲的兔子們。

不管未來是怎麼樣，希望這幾年的學習和經驗，都能轉化成為我向前的力量。再次謝謝大家，僅以此論文和你們分享。

Table of Contents

1. Introduction

1.1 Classical receptive field of retinal ganglion cells in vertebrate retina

In vertebrate retina, five major types of neurons form a three-layer neural network which is composed of the vertical pathway (photoreceptors to bipolar cells to ganglion cells) and the lateral pathway (horizontal cells in the outer retina, and amacrine cells in the inner retina). Among these neurons, retinal ganglion cells (RGCs) are final output neurons that convey visual information to higher visual centers in the brain. Furthermore, RGCs can be classified into 10-15 different types based on their dendritic features in the mammalian retina. Besides the morphological difference, their physiological responses to light stimulation are also different (Masland, 2001; Wassle, 2004). In particular, the receptive field of RGCs, the region on the retina where a neuron could be evoked by light stimulation (Hartline, 1938), exhibits cell type specific properties. Antagonistic concentric receptive fields, namely the ON center/OFF surround and the OFF center/ON surround, were described early by Kuffler (1953). More complex receptive fields of RGCs have also been reported. For instance, the direction selective ganglion cells (DSGCs) in the rabbit retina respond to a bar moving in certain direction vigorously, but show little or no response when a bar moves in the opposite direction (Barlow & Hill, 1963; Barlow et al., 1964).

1.2 Spatiotemporal receptive field of retina ganglion cell

In addition to these classical mapping approaches, receptive field microstructures in both space and time domain have been revealed when white noise stimuli were applied to characterize RGCs in vertebrate retinas. White noise is a set of stimulation that provides easily interpretable model of light responses, even if the neuronal response itself is nonlinear. This stimulus is made of a set of flickering checkerboard patterns containing light and dark squares, where each element in each frame is modulated independently by using a pseudorandom sequence (Reid et al., 1997). The final output of the white noise procedure is a spike triggered average (STA), which is taken by calculating the reverse correlation between neural response and stimuli. Put another way, STA is a movie containing both spatial and temporal receptive fields of a given RGC (Chichilnisky, 2001). On the temporal aspect, STA is a stimulus intensity as a function of time that represents the average effective stimulus preceding the occurrence of a spike (Devries & Baylor, 1997). In space domain, however, each frame of STA illustrates the microstructure of RGCs' spatial receptive field at given time point. Previous studies have shown that the receptive field profiles of RGCs are more irregular with several regions having higher sensitivity (Chichilnisky & Baylor, 1999; Brown et al., 2000), unlike the spatial organization of RGC receptive field typically described as dorm-shaped like by a difference of Gaussians function.

1.3 Development of retinal ganglion cells in the rabbit retina

The development of retina has been a great of interest for long time, because its importance in vision and its competence for neural system inquiry (Wong & Godinho, 2003). Previous research in uncovering developmental mechanisms of RGCs indicates gradual changes in dendritic pattern and physiological maturity. Specifically, the dendrites of RGC have an excess of dendritic spines and branches that are gradually reduced. This process spans the first three weeks in neonatal rabbit, and the remodeling pattern is different among different RGC types (Amthor et al., 1984; Amthor et al., 1989a, b; Wong, 1990; Deich et al., 1994). On the other hand, previous experiments indicate that the receptive field properties of rabbit RGCs, such as concentric center-surround receptive field and the direction selectivity, can be detected around eye opening at postnatal day 10 (P10) and become mature as adult at P21 (Bowe-Anders et al., 1975; Masland, 1977). However, the result of electroretinogram shows that retinal function is immature until the rabbit has reached five weeks of age (Reuter, 1976; Gorfinkel et al., 1988). In all these classical experiments, RGCs were coarsely categorized into merely 2 to 4 classes by their dendritic morphology or concentric receptive field. However, the classifications of adult rabbit RGCs based on physiological and morphological features are much clear

today. For example, there is a recent study in which the complex RF properties of the rabbit ON-OFF DSGCs have been shown to be modulated after eye opening. Particularly, the direction selectivity, velocity tuning, center-surround organization, and motion surround inhibition induced by preferred direction in ON-OFF DSGCs, all gradually mature after P10 and become adult-like until P22 (Chan & Chiao, 2008). Furthermore, previous results from the electron microscopic study show that conventions and ribbon synapses in the inner plexiform layer of developing rabbit retina general increase between P9 and P20 (McArdle et al., 1977). Taken together, dendritic and receptive fields of neonatal rabbit RGCs appear to develop continuously after eye opening.

1.4 Goals and summary

The primary goals of this study are to investigate the physiological and morphological properties of ON and OFF alpha RGCs throughout development after eye opening in rabbits, and to examine the correlation between dendritic pattern and receptive field maturation. We found that temporal resolution and integration capacity in the receptive fields of alpha RGCs gradually matured from stage P10-14 to P20-23, and from P20-23 to adult. On the contrary, the robustness of response to light in alpha cells did not reach to the adult level until postnatal week three, and the alteration

seems to be relatively abrupt. Although the variation of spatial resolution and dendritic densities in alpha RGCs is slightly larger at stage P10-14, there is no apparent difference among age groups. Moderate correlation between the receptive field sensitivities and dendritic densities could be observed during development, however, the correlation showed apparent fluctuations within each developmental group of alpha RGCs. Overall, our results indicate that some physiological properties of ON and OFF alpha RGCs still develop after eye opening in rabbits, but the correlation between morphology and physiology of alpha RGC does not show a consistent developmental pattern.

2. Materials and Methods

2.1 Retina preparation

New Zealand White rabbits were either bred in the Laboratory Animal Room of BEC National Tsing Hua University, or purchased from a local breeder. The day of neonate's birth is designated as P0 (postnatal day 0), and the three groups of rabbits at different developmental stages used in this study were P10-14, P20-23, and adult (1 to 2 kg). All procedures were approved by the institutional animal care and use committee and were in accordance with the ARVO Statement for Use of Animals in Ophthalmic and Vision Research.

To label nuclei of retinal neurons, rabbits were anesthetized with a mixture of ketamine (75 mg/kg) and xylazine (15 mg/kg) 1-2 days before the experiment. After application of topical anesthetics 0.5% proparacaine hydrochloride ophthalmic solution (Alcaine; Alcon-Couvreur, Belgium), 2-3 μl of 4', 6-diamidino-2-phenylindole (DAPI; 1 μM, Sigma, St. Louis, MO, U.S.A.; #D-9542) was injected intraocularly. On the day of the experiment, the animal was dark adapted for at least one hour and then deeply anesthetized with intramuscular injection a mixture of ketamine (150 mg/kg) and xylazine (30 mg/kg), and following topical anesthesia of Alcaine application on its eyes. Dissection proceeded under dim red light. After enucleation, lens and vitreous were removed from the hemisected eye ball,

and the posterior eye cup was everted and hanged over the round head of a Teflon rod, which was immersed in the oxygenated Ames medium (Sigma, #A1420; Ames & Nesbett, 1981) or modified Ames medium (120 mM NaCl, 3.1 mM KCl, 0.5 mM KH_2PO_4, 1.2 mM $MgSO_4$, 1.15 mM $CaCl_2$, 6.0 mM D-glucose) containing 23mM $NaHCO_3$. Retina was carefully isolated from the retinal pigment epithelium. The rabbit was euthanatized by CO_2.

The piece of retina was affixed photoreceptor-side down on a coverslip coated with tissue adhesive (Cell-Tak; BD Biosciences, Bedford, MA; #354240). This preparation was transferred to a recording chamber mounted on the stage of a fluorescence microscope (Axioskop 2 FS Plus, Zeiss, Germany), and superfused with Ames medium (1.5-2 ml/min) at 34-37 °C.

2.2 Visual Stimuli

Visual stimuli generated by the VisionWorks (Vision Research Graphics, Durham, NH) were displayed on a CRT monitor (refresh rate 60 Hz; SyncMater 757NF; Samsung, Korea) and reflected upward by a mirror positioned beneath the microscope stage. A 20× microscope objective (A-plan, NA 0.45, Zeiss) replaced the condenser of microscope was used to focus the stimulus onto the photoreceptor layer of the retina (Fig. 1A).

The following visual stimuli were used to investigate the receptive field properties of the alpha RGCs during the development. First, the alpha RGCs had typical brisk transient burst ON or OFF response to a flashing light square (Cleland & Levick, 1974). Second, the center-surround interaction was studied by displaying a short duration (167 ms) of flashing circles with different diameters centered at the receptive field center (Cleland & Levick, 1974). Third, a binary white noise stimulus (a 400 μm square randomly flickering at 60 Hz) was used for examining the temporal characteristics in the receptive field center of RGCs. Fourth, the spatiotemporal receptive fields of RGCs were detected with a flickering checkerboard composed of either 8×8 or 16×16 black/white squares (Fig. 1C and 1D). Stimulus refresh rate was 60 Hz, thus the display duration of each frame was ~17ms, and the time of one trial was 30-120 sec. Every time the stimulus frame refreshed, the intensity of each square was modulated independently and determined by a pseudorandom sequence (Reid et al., 1997). The width of the squares in checkerboard on the side of retina was about 110 to 240 μm, equivalent to a half or one-third of the RGC's receptive field center diameter. Luminance values of stimuli on the stage ranged from 0.01cd/m^2 to 15 cd/m^2 and generally fell within the mesopic range.

2.3 Extracellular recording

RGCs labeled with DAPI were visualized under brief fluorescence illumination (365 nm excitation) using a 40× water immersion objective (Achroplan, NA 0.8, Zeiss). Most recordings were obtained from the RGCs with large somas located at central and mid-peripheral regions of the retina (Peichl et al., 1987). The activity of single ganglion cells was recorded with the tungsten-in-glass electrode (Levick, 1972), which had an impedance range of 0.8-1.8MΩ. The neural signal was amplified 1000 folds and band-pass filtered at 100 Hz-3 kHz with a differential amplifier (ISO-80; World Precision Instruments, Sarasota, FL). A data acquisition system including an analog-to-digital acquisition card (NI 6040E; National Instruments, Austin, TX) and LabView program (National Instruments) was used to record neuronal signals with the 10 kHz sampling rate by a computer for latter offline analysis.

2.4 Intracellular dye injection

After recording, the tungsten-in-glass electrode was withdrawn and replaced by a micropipette pulled from the thick-wall borosilicate glass capillaries with filament (o.d. = 1.0 mm, i.d. = 0.5 mm; Sutter Instrument, Novato, CA, #BF1005010) using a programmable Flaming-Brown P97 puller (Sutter Instrument) for intracellular dye injection. The micropipette was filled with 2% Lucifer Yellow (Sigma, #861502) and

4% N-(2-aminoethyl)-biotinamide hydrochloride (Neurobiotin; Vector Laboratories, Burlingame, CA; #SP1120) in 0.1M Tris buffer. An intracellular amplifier (Neuroprobe Amplifier 1600, A-M Systems, Carlsborg, WA) was used to perform the iontophoresis with biphasic current (1-2 nA) for 1-2 minutes. For subsequent alignment between RGC's dendritic arbor and the stimulus, the soma and proximal dendrites of the neuron were immediately photographed at 40× magnification using a digital camera (Coolpix P5100, Nicon). Subsequently, the retina was fixed in 4% paraformaldehyde (in 0.1 M PB) for 40 minutes. The injected cells were then visualized by incubating the retina with a FITC-conjugated streptavidin (diluted 1:50 in 0.1M PB with 0.1% Triton X-100; Sigma; #SA5001) at room temperature overnight. The retina was flat-mounted in the mounting medium (Vectashield; Vector Laboratories, Burlingame, CA; #H1000) for imaging under a confocal microscope.

2.5 Image acquisition

Images of the injected cells were acquired using a laser scanning confocal microscope (LSM 5 Pascal, or LSM 510 Pascal, Zeiss) with a 20× objective lens (Plan-NEOFLUAR, NA 0.5, Zeiss) or a 40× objective lens (Plan-NEOFLUAR, NA 0.75, Zeiss), depending on the dendritic field size. A series of z-stack images was taken from the focal plane of axon terminals to the focal plane that included ON or

OFF dendritic arbors of alpha RGCs. A LSM 5 image examiner (v3.1.0.99, Zeiss) was used to adjust image intensity and contrast.

2.6 Data analysis

Offline data analysis was carried out using the MATLAB software (The MathWorks Inc, Natick, MA) and programs developed in-house. To reveal the strength of inhibitory surround in RGC receptive field, we calculated the inhibition strength index (ISI), which was simply the difference between the strongest and the weakest normalized responses to circle stimuli with varied diameters. That is, the surround suppression to the center-along response of excitatory receptive field center. Thus, an ISI value close to 1 represents strong surround inhibition (Chan & Chiao, 2008). Neural responses were extracellular recorded spike train of RGCs binned at ~17ms depending upon the stimulus refresh rate. Sequences of stimulus patterns were reverse correlated to the neural response for computing the consequent spike triggered average (STA). STA is a stimulus profile with unit of light intensity, which is normalized between -1 and +1 (Fig. 1). Further, it is a function of space and time to exhibit the average stimulus preceded the occurrence of spikes, and to represent the spatiotemporal receptive fields of RGCs (Devries & Baylor, 1997; Chichilnisky, 2001). The average temporal STA of individual RGC was obtained from 3-4 trials and

smoothed by cubic spline interpolation. Figure 3A illustrates the chosen parameters of temporal STA used for successive comparison. In Figure 4, the spatial receptive field was defined as the STA frame with the maximal pixel by pixel intensity value summation in an entire serious of spatiotemporal STA (Appendix 2). To demonstrate the spatial profile of STA, pixels with the averaged stimulus intensity values exceeding mean±1 SD were considered significant and color coded for manifest visualization. Other pixels were displayed in gray scale; however, both color and gray gradations are according to normalized intensities. Figure 5A illustrates the parameters of spatiotemporal STA used for advanced comparison. In order to inspect the correlation between physiology and morphology properties of RGCs, the camera lucida of RGC dendrites was depicted from confocal images and aligned with the spatial STA. Dendritic densities came from RGCs confocal images processed by Photoshop software (Photoshop; Adobe Systems, Mountain View, CA) and image pixels calculation by Matlab program.

Statistical analyses were performed using SAS (SAS Institute Inc., Cary, NC). For unbalanced data, we evaluate the parameters of temporal and spatiotemporal STA with a general linear model to disclose the difference between differ developmental groups. We also calculated the Pearson's correlation coefficient between the values of spatial STA and dendritic densities to reveal their correlation. For this study, a value

of $p < 0.05$ was considered significant.

3. Results

In all experiments, alpha ganglion cells in the mid-peripheral region of the rabbit retina at three different development stages were first targeted under microscope. The alpha ganglion cell was recognized by its oval nucleus prestained with DAPI and by its relative large soma (about 20um in diameter). We used the tungsten-in-glass electrode (Levick, 1972) to carry out the single cell extracellular recording of these ganglion cells. Alpha ganglion cells had either ON or OFF transient response to the flash light stimulus (Cleland & Levick, 1974). During development, it has been reported that some retinal ganglion cells (RGCs) have silent surround or absent surround at around eye opening in the rabbits (Masland, 1977). The whole field temporal-varied white noise stimuli were presented in the receptive field center of alpha RGCs, and the size was determined by manual receptive field mapping. To verify the spatial extent of the manually mapped receptive field, a brief flash of a circle (167 ms) with various diameters was used to evoke light response. The results showed that the width of the whole field white noise stimuli were about 1-2.5 times of the diameter of the light flash that induced the strongest response for the same alpha RGCs (see Appendix 1C and 1D). We reasoned that the width of the white noise stimuli used in this experiment is appropriate, because the diameters of circular stimuli tend to underestimate the spatial extent of the RGC receptive field. We further

characterized the magnitude of surround inhibition by the inhibition strength index (ISI) (Chan & Chiao, 2008). In our results, the ON alpha cells had slightly stronger surround inhibition than the OFF alpha cells (Appendix 1A and 1B), thus the ISI of the ON alpha cells was higher than the OFF alpha cells (Appendix 1C and 1D). Note that these ISIs did not vary from P10-14 stage to Adult.

3.1 Temporal STA of ON and OFF alpha cells show broader time course pattern and lower STA value before P20

Consistent with previous studies (Devries & Baylor, 1997; Brown et al., 2000), the temporal STA results of using the whole field white noise stimuli showed biphasic waveform pattern. Specifically, the upward and downward lobe of temporal STA were typical with similar amplitudes in the ON alpha cells (Fig. 2E), but the upward lobe was smaller than the downward one in the OFF alpha cell (Fig. 2F). These characteristics are in accordance with the mean effective stimulus time courses of ON and OFF brisk transient RGCs found in adult rabbits (see (Devries & Baylor, 1997). We also found that the temporal STA integration time of adult rabbit ON and OFF alpha cells were about 200 ms (Fig. 2E and 2F). The integration time (Fig. 3A) represents the duration in which stimuli change intensity before triggering a spike. We showed that ON and OFF alpha cells from stage P20-23 had longer integration time

(nearly 400 ms) than adult stage (Fig. 2C and 2D). The STA of P10-14 alpha cells had even longer integration time approximately 500 ms (Fig. 2A and 2B). This suggests that immature alpha cells could not response to the light intensity variation occurring in a short time interval. Moreover, by carefully examining the temporal STA results, the time before reaching the first peak is informative (see t1 in illustration of Fig. 2A and Fig. 5A), and can be used to represent the spatial receptive field of RGC (Devries & Baylor, 1997; Brown et al., 2000). Comparing to previous observations in adult rabbit alpha RGCs, the t1 of temporal STA profile from adult rabbit alpha RGCs varies from -190 ms to -71 ms (Devries & Baylor, 1997; Brown et al., 2000), and it was -90 ms to -70 ms in our results (Fig. 2E and 2F). These variations might be due to different experiment conditions and particularly the light intensities. Devries and Baylor (1997) have suggested that the t1 is reduced when the light intensity is increased. Thus, we had done experiments on alpha RGCs by varying the levels of intensity from 1 to 15 cd/m^2 to confirm this possibility. In P10-14 alpha cells, t1 was -150 ms to -130 ms (Fig. 2A and 2B), and it was ~ -100 ms in P20-23 alpha cells (Fig. 2C and 2D).We discovered that the absolute value of temporal STA peak one was coarsely lower for ON and OFF alpha cells at respective stage P10-14 than P20-22 and adult (Fig. 2A-F).

3.2 Characteristics of temporal STA of ON and OFF alpha cells changed during development reveal functional maturation of retina

Considering foregoing interpretation, we investigated several characteristics mentioned above of temporal STA from ON and OFF alpha cells population at three developmental stages. Representative temporal STA and its characteristics were demonstrated (Fig. 3A). Spike rates of RGCs may affect the pattern of temporal STA. In our result, the spike rates were not different between ON and OFF alpha cells for various developmental groups (Fig. 3B). The absolute values of temporal STA from ON alpha cells significant increased from P10-14 to adult (Fig. 3C; p = 0.048) for about 44%. The t1 was different among the first two stages and adult (Fig. 3E; p = 0.001 for P10-14 vs. adult; p = 0.011 for P20-23 vs. adult). T1 reduced from P10-14 (mean = -127 ms) to P20-23 (mean = -116 ms), then to adult (mean = -93 ms) (Fig. 3E, and Table 1). The t2 was different only in P10-14 and adult (Fig. 3E; p = 0.011).

Temporal STA of OFF alpha cells showed that the absolute values of STA were different between P10-14 and the other two stages (Fig 3D; p = 0.025 for P10-14 vs. P20-23; p = 0.029 for P10-14 vs. Adult), and it increased 29% after P20. The t1 and t2 also changed throughout development of OFF alpha cells. The t1 gradually decreased (Fig. 3F; p < 0.0001 for P10-14 vs. P20-23; p <0.0001 for P10-14 vs. adult; p = 0.027 for P20-23 vs. adult). The t1 reduced from -162 ms to -113 ms, then to -93 ms. The

integration time of P10-14 was longer than the other two stages (Fig. 3F; p = 0.044 for P10-14 vs. P20-23; p = 0.005 for P10-14 vs. adult). Taken together, the raised values of STA suggest that matured alpha cells have robust response to light stimulation. On the other hand, the decreasing t1 and t2 in temporal STA suggests that matured alpha cells can detect faster and more subtle fluctuations of light signals. It is interesting that the absolute value of STA mainly increased after P20 in both ON and OFF alpha cells, there was no further increase between P20-23 stage and adult. Nonetheless, the time course of temporal STA changed from a broader pattern to a shaper one was a gradual process during the development. These results imply that there might be different underlying mechanisms responsible for functional maturation of ON and OFF alpha RGCs.

3.3 Spatiotemporal STA of ON and OFF alpha cells at different developmental stages

The morphology of rabbit alpha RGC undergoes remodeling such as reduction of spines and number of nodes even after eye opening in the rabbit (Wong, 1990), but whether remodeling influences physiological function of the developing RGC is not clear. Therefore, we used white noise stimuli to investigate the spatiotemporal receptive field of alpha RGCs during development, and injected the cells with Lucifer

yellow after recording to obtain the morphology of RGCs. After determining the effective configurations from the serial spatiotemporal STA (see the methods and Appendix 2), spatial STA profiles could be aligned to the dendritic pattern of the RGCs. The results showed that there were several pixels (the mosaic squares in STA profile) with STA values greater than one standard deviation of STA values in each frame. If these pixels clustered within the extent of dendritic arbor drawn from ON or OFF alpha cells, they were considered as effective pixels. Based on this criterion, the STA profile contained 4 to 5 effective pixels at P10-14 (Fig. 4A and 4D). However, the number of effective pixels was 5-6 in STA at P20-23 (Fig. 4B and 4E), and went up to 6-9 in STA profile of adult RGCs (Fig. 4C and 4F). This trend of increasing effective pixels is accompanied by maturation of the RGCs. At all development groups, the fluctuation of STA values indicates that sensitivities of small regions in the receptive field of RGC were inhomogeneous, known as the receptive field microstructure (Brown et al., 2000). Besides, there were several pixels with the inverse sign of STA surrounded the receptive field center, suggesting the expression of the antagonistic center-surround structure of RGC classic receptive field. Consistent with temporal STA, the spatial STA center and surround at t1 and t2 showed reverse phases. Subtle different STA features could be found at distinct time points. For instance, pixels that had highest absolute value of STA located differently

in spatial t1 and t2 STA profiles (Fig. 4A - F).

Inspecting the time domain of spatiotemporal STA, we found that the t1 of ON and OFF alpha RGCs reduced during development. From P10-14 stage to P20-23 and then to adult, the t1of ON RGCs was - 118 ms to - 85 ms and then - 85 ms. The t1 of OFF RGCs was - 119 ms to - 102 ms then to - 83ms. On the contrary, the t2 did not have such trend (Fig. 4A - F).

3.4 Characteristics of spatiotemporal STA of ON and OFF alpha cells alter during development

Referring to the spatiotemporal STA results from different population through development, we examined several parameters of the STA (Fig. 5A). Given white noise stimuli, the spike rates of ON and OFF alpha RGCs from different developmental groups had no difference (Fig.5B). We also tested if alpha RGCs would have different spatial resolution for this mapping method at each age group. In spatiotemporal STA trials, 8 by 8 white noise stimuli with various widths were used. However, alpha cells from three stages showed no apparent different responses to these stimuli. At stage P10-14, the t1 effective STA summation had large variation, and there was a trend of increasing STA sum (Fig. 5C and 5D). The t2 effective STA summation did not vary with an obvious pattern (Fig. 5C and 5D), but there was

significant difference between t2 STA sum of P10-14 and P20-23 ON alpha cells (Fig. 5C; $p = 0.043$).

Only t1 from spatiotemporal STA of ON alpha cells was longer in immature P10-14 and P20-23 alpha RGCs than in the matured ones (Fig. 5E; $p = 0.0001$ for P10-14 vs. adult; $p = 0.015$ for P20-23 vs. adult). From the three age groups, t1 of ON alpha was shortened from - 127 ms to - 119 ms, and then to -88 ms. In contrast, both t1 (Fig. 5F; $p < 0.0001$ for P10-14 vs. P20-23; $p < 0.001$ for P10-14 vs. adult) and t2 (Fig. 5F; $p = 0.013$ for P10-14 vs. adult; $p = 0.010$ for P20-23 vs. adult) of OFF alpha cells were shortened from P10-14 till adult. The transition of the t1 and t2 for OFF alpha cells were - 166 ms to -110 ms to - 88 ms, and - 393 ms to - 319 ms to - 299 ms, respectively.

3.5 Correlation between spatial STA values and dendritic densities of developing ON and OFF alpha RGCs

Previous research shows that the mass center of the receptive field computed from the spatial STA profile is not coincided with the soma of rabbit alpha RGC in spite of their nearly symmetric morphology (Brown et al., 2000). Given the fact that dendritic pattern remodeling is continued until maturation in alpha RGCs (Wong, 1990; Deich et al., 1994), we attempt to examine the alteration of the physiological

and morphological properties during retinal development. The dendritic densities resulted from dendritic pattern of alpha RGCs were compared to the values within the spatial STA profiles at corresponding regions (see methods and Appendix 2). In general, the scatter plots showed that both ON and OFF cells dendritic field covered regions with plus and minus STA values. However, higher dendritic densities correlated with larger STA values with inphase signs, that is, plus for ON cells and minus for OFF cells (Fig. 6). The correlation coefficients between dendritic densities and STA values fluctuated, and they did not show a clear trend correlating with development (Table 1). To compare only the correlation coefficients with statistical significance, ON and OFF alpha RGCs at stage P20-22 had little higher correlation coefficients (Fig. 6B and 6D, Table 1). Dendritic densities and STA values had great variation in several single cells at stage P10-14 (data points with large error bars in Appendix 3). Among P10-14 alpha cells, there was also divergence in population data. The mean values of dentritic densities and STAs of P10-14 were either lower or higher than those values came from P20-22 or Adult alpha cells (dispersive P10-14 data points in Appendix 3).

4. Discussions

4.1 Temporal properties of STA in alpha RGCs that gradually develop after eye-opening correlate with the maturation process of the ribbon synapses in relaying excitatory signals in the retina

In the present study, we found that temporal features of STA of alpha RGCs gradually changed during development. RGC had slower peaked times (t1 and t2) and longer stimulus integration time at P10-14 than in adult (Fig. 2, Fig. 3E and 3F). It implies that immature alpha RGCs have worse temporal resolution of light stimuli. In other words, they could not respond well to the sudden change of light intensity. This result is in accordance with the studies in kitten that the brisk ganglion cells played poor temporal resolution to some fast stimuli (a 0.75Hz flashing spot) around eye opening (Tootle, 1993). Furthermore, it has also been reported that the time course of RGC spatiotemporal receptive fields in adult frogs was as twice fast as that in tadpoles (Shingai et al., 1983).

One possibility to account for these gradual changes of temporal STA properties during the development of rabbit RGCs is that the ribbon synapse continues to develop after eye-opening. In the developing rabbit retina, it is known that the amount of ribbon synapses in the OPL significantly increases about 2 days before eye-opening at around P9-10. However, the ribbon synapse density abruptly increases in the IPL

after P9-10, and the ribbon synapse structural assembly in both the OPL and IPL would not reach the mature level until P18 (McArdle et al., 1977). Despite the structure and function of ribbon synapses in the adult mammalian retina are well studied (Sterling & Matthews, 2005; tom Dieck & Brandstatter, 2006), their functional roles in retinal circuit development is less clear. Ribbon synapse transmits signals from the photoreceptors to the bipolar cells, and the bipolar cells also send their outputs to the ganglion cells using the same ribbon synapses (Wassle, 2004). Its fast release of neurotransmitter glutamate within 1-2 ms is essential in the vertical excitatory pathways of the retina (Heidelberger et al., 1994; tom Dieck & Brandstatter, 2006). In a recent study, the *pikachurin* (a ribbon synapse related protein) mutant mice had a defect of forming normal ribbon synapse in bipolar cells, and showed abnormal ERG b-waves and optokinetic responses (Sato et al., 2008). This finding indicates that ribbon synapse is necessary for normal retinal function, and that ERG b-wave is attributable to neural activities of ON bipolar cells and inner retina (Gurevich & Slaughter, 1993; Dong & Hare, 2000). Moreover, there are evidences showing that peak time and amplitude of ERG b-waves in the rabbit retina vigorously changed to adult level within 2 to 3 weeks after birth (Reuter, 1976; Gorfinkel et al., 1988; Gorfinkel & Lachapelle, 1990). In our current results, we also found variations of temporal STA characteristics throughout the development of rabbit retina after

eye-opening. Since the white noise stimulation for temporal STA in our study was spatially static, the excitatory instead of inhibitory mechanism is more plausible. Additionally, there is a recent report indicating that the excitatory pathways still develop in the mouse retina after eye-opening (Elstrott et al., 2008). Taken together, we think it is likely that the variations in temporal STA reflect the maturation states of ribbon synapse in the developing rabbit retina.

4.2 Strength of STA increasing at P20-23 stage implies that the robustness of alpha RGC response to light stimulation is developmentally modulated

According to our results, it was found that the maximum value of temporal STA is not unity, and the minimum value is not minus one either (Fig. 2, Fig. 3C and 3D). Based on the cross-correlation algorithm of computing STA and the fact that the stimuli used in our experiments were binary, the reason that the strength of STA is away from unity is likely resulting from some uncorrelated spikes whose occurrence is not correlated with stimuli. In other words, the spontaneous firing of RGCs would render the absolute value of STA deviate from the unity. We showed that the absolute value of temporal STA was lower for alpha cells at stage P10-14 than adult, but there was no difference between stage P20-23 and adult (Fig. 3C and 3D). This indicates that alpha cells yet completely developed might have more spontaneous spikes, a

result consistent with the finding in developing rabbit retina (Masland, 1977). On the contrary, the previous studies in mouse and cat showed that spontaneous firing rate of immature RGCs is lower than that in matured ones (Tootle, 1993; Tian & Copenhagen, 2001). The fact that the firing rates of ON and OFF alpha RGCs at different development stages in our experiments were not significant different (Fig. 3B), other underlying mechanisms must contribute to the higher spontaneous spikes in immature alpha RGCs. For instance, it has been shown that DSGCs from neonatal mouse have lower membrane excitability, lower reliability of synaptic transmission, and slower kinetics of light responses (Chen et al., 2009). The rabbit bipolar cells have lower membrane potential variation while stimulated by light, and this physiological property becomes adult-like after P16 (Dacheux & Miller, 1981). Since immature cellular mechanisms typically generate spikes with longer latency, the absolute value of STA would be susceptible to time variation of spikes.

4.3 Different results of temporal STA and spatiotemporal STA show possible variant temporal and/or spatial properties in alpha RGC receptive fields

The results of temporal STA and spatiotemporal STA from developing ON and OFF rabbit alpha cells are somewhat different. The temporal STA values of alpha RGCs approached the matured level after P20, but that did not consistently occur in

the spatiotemporal STA summation (Fig. 3C, 3D, 5C, and 5D). Although the decreasing trend of peak (t1, t2) and integration time in temporal STA and spatiotemporal STA were collateral, only tl of ON alpha and t2 of OFF alpha RGCs in spatiotemporal STA results showed this trend, and these parameters in temporal STA reduced gradually from P10-14 to P20-23 then to mature level of adult. Furthermore, these peak times were even shorter in spatiotemporal STA than in temporal STA (Fig. 3E, 3F, 5E, and 5F). Since the white noise stimuli for getting temporal STA was uniform in spatial dimension, but was spatially varied in spatiotemporal STA, retinal circuitries for integrating light stimuli with different spatial scales might contribute to these differences between temporal and spatiotemporal STA results.

4.4 Moderate correlations between spatial STA values and dendritic densities of ON and OFF alpha RGCs do not change throughout different developmental stages

Although previous studies showed that the dendritic fields of alpha cells exhibit extensive remodeling, including dramatic increase of the number of spines, nodal points, and the intermodal distance during development of rabbit retinas (Amthor et al., 1984; Amthor et al., 1989a, b; Wong, 1990; Deich et al., 1994), there is no direct evidence correlating the morphological and physiological properties at the same time.

In this study, the spatial STA profiles representing the subtle sensitivity distribution in RGC receptive fields were compared with RGC dendritic patterns directly. The correlation coefficients between dendritic densities and spatial STA were moderate for all three different developmental stages (Fig 6, and Table 1). This is in accordance with previous observation that there is no predictable relation between dendritic arbors and receptive field microstructures (Brown et al., 2000). In our study, dendritic densities were calculated in corresponding spatial STA grids with similar width. Examining first the dendritic densities among different age groups, we found that several P10-14 alpha cells have mean dendritic densities higher than that in P20-23 and adult ones (Appendix 3). It has been shown that the main remodeling feature of dendritic arbor in developing of alpha cells is interstitial, which means elongation of dendrite length between nodes (Wong, 1990; Deich et al., 1994). In considering the properties of spatiotemporal STA, it has also been suggested that spatial distribution of bipolar cell axon synapsed on ganglion cell dendrites might contribute to the receptive field anisotropism (Brown et al., 2000). Furthermore, another recent study reported that the spatial distribution pattern of glutamatergic inputs on dendritic arbors of adult rabbit RGCs is surprisingly with little variation and is independent of RGC categories. However, RGC with smaller size of dendritic field would have higher densities of synaptic inputs (Jakobs et al., 2008). Size of dendritic field of

alpha RGC was increased evidently during development in previous studies (Wong, 1990; Deich et al., 1994) and in our observations (Fig. 4). The fact that the correlations between dendritic densities and STAs are only slightly different among P10-14, P20-23, and adult alpha cells (Fig. 6) indicates that the input strength onto dendrites of alpha RGCs may be constant during development.

It is unclear whether the growth of bipolar cell axonal terminals is proportional or disproportional to the growth of ganglion cells (Deich et al., 1994). It is possible that alteration of spatial extent of receptive fields of bipolar cells, additional amount of synapse connection between bipolar cells and ganglion cells, or adjustment of synapse strength (ribbon synapse maturation) might contribute to underlying mechanisms affecting the input strength during development (Fig. 7). Thus, future researches about distribution pattern of synaptic inputs on developing RGCs, spatiotemporal receptive field changes of upstream neurons, and the structural and functional maturation of ribbon synapses in the inner and outer retinas are crucial to elucidate the plasticity of neural circuitry in the developing retina and the correlation between structure and function of these various retinal ganglion cells.

5. References

Ames A, 3rd & Nesbett FB. (1981). In vitro retina as an experimental model of the central nervous system. J Neurochem 37, 867-877.

Amthor FR, Oyster CW & Takahashi ES. (1984). Morphology of on-off direction-selective ganglion cells in the rabbit retina. Brain Res 298, 187-190.

Amthor FR, Takahashi ES & Oyster CW. (1989a). Morphologies of rabbit retinal ganglion cells with complex receptive fields. J Comp Neurol 280, 97-121.

Amthor FR, Takahashi ES & Oyster CW. (1989b). Morphologies of rabbit retinal ganglion cells with concentric receptive fields. J Comp Neurol 280, 72-96.

Barlow HB & Hill RM. (1963). Selective sensitivity to direction of movement in ganglion cells of the rabbit retina. Science 139, 412-414.

Barlow HB, Hill RM & Levick WR. (1964). Retinal Ganglion Cells Responding Selectively to Direction and Speed of Image Motion in the Rabbit. J Physiol 173, 377-407.

Bowe-Anders C, Miller RF & Dacheux R. (1975). Developmental characteristics of receptive organization in the isolated retina-eyecup of the rabbit. Brain Res 87, 61-65.

Brown SP, He S & Masland RH. (2000). Receptive field microstructure and dendritic geometry of retinal ganglion cells. Neuron 27, 371-383.

Chan YC & Chiao CC. (2008). Effect of visual experience on the maturation of ON-OFF direction selective ganglion cells in the rabbit retina. Vision Res 48, 2466-2475.

Chen M, Weng S, Deng Q, Xu Z & He S. (2009). Physiological properties of direction-selective ganglion cells in early postnatal and adult mouse retina. J Physiol 587, 819-828.

Chichilnisky EJ. (2001). A simple white noise analysis of neuronal light responses. Network 12, 199-213.

Chichilnisky EJ & Baylor DA. (1999). Receptive-field microstructure of blue-yellow ganglion cells in primate retina. Nat Neurosci 2, 889-893.

Cleland BG & Levick WR. (1974). Brisk and sluggish concentrically organized ganglion cells in the cat's retina. J Physiol 240, 421-456.

Dacheux RF & Miller RF. (1981). An intracellular electrophysiological study of the ontogeny of functional synapses in the rabbit retina. I. Receptors, horizontal, and bipolar cells. J Comp Neurol 198, 307-326.

Deich C, Seifert B, Peichl L & Reichenbach A. (1994). Development of dendritic trees of rabbit retinal alpha ganglion cells: relation to differential retinal

growth. Vis Neurosci 11, 979-988.
Devries SH & Baylor DA. (1997). Mosaic arrangement of ganglion cell receptive fields in rabbit retina. J Neurophysiol 78, 2048-2060.
Dong CJ & Hare WA. (2000). Contribution to the kinetics and amplitude of the electroretinogram b-wave by third-order retinal neurons in the rabbit retina. Vision Res 40, 579-589.
Elstrott J, Anishchenko A, Greschner M, Sher A, Litke AM, Chichilnisky EJ & Feller MB. (2008). Direction selectivity in the retina is established independent of visual experience and cholinergic retinal waves. Neuron 58, 499-506.
Gorfinkel J & Lachapelle P. (1990). Maturation of the photopic b-wave and oscillatory potentials of the electroretinogram in the neonatal rabbit. Can J Ophthalmol 25, 138-144.
Gorfinkel J, Lachapelle P & Molotchnikoff S. (1988). Maturation of the electroretinogram of the neonatal rabbit. Doc Ophthalmol 69, 237-245.
Gurevich L & Slaughter MM. (1993). Comparison of the waveforms of the ON bipolar neuron and the b-wave of the electroretinogram. Vision Res 33, 2431-2435.
Heidelberger R, Heinemann C, Neher E & Matthews G. (1994). Calcium dependence of the rate of exocytosis in a synaptic terminal. Nature 371, 513-515.
Jakobs TC, Koizumi A & Masland RH. (2008). The spatial distribution of glutamatergic inputs to dendrites of retinal ganglion cells. J Comp Neurol 510, 221-236.
Kuffler SW. (1953). Discharge patterns and functional organization of mammalian retina. J Neurophysiol 16, 37-68.
Levick WR. (1972). Another tungsten microelectrode. Med Biol Eng 10, 510-515.
Masland RH. (1977). Maturation of function in the developing rabbit retina. J Comp Neurol 175, 275-286.
Masland RH. (2001). The fundamental plan of the retina. Nat Neurosci 4, 877-886.
McArdle CB, Dowling JE & Masland RH. (1977). Development of outer segments and synapses in the rabbit retina. J Comp Neurol 175, 253-274.
Peichl L, Buhl EH & Boycott BB. (1987). Alpha ganglion cells in the rabbit retina. J Comp Neurol 263, 25-41.
Reid RC, Victor JD & Shapley RM. (1997). The use of m-sequences in the analysis of visual neurons: linear receptive field properties. Vis Neurosci 14, 1015-1027.
Reuter JH. (1976). The development of the electroretinogram in normal and light-deprived rabbits. Pflugers Arch 363, 7-13.
Sato S, Omori Y, Katoh K, Kondo M, Kanagawa M, Miyata K, Funabiki K, Koyasu T, Kajimura N, Miyoshi T, Sawai H, Kobayashi K, Tani A, Toda T, Usukura J,

Tano Y, Fujikado T & Furukawa T. (2008). Pikachurin, a dystroglycan ligand, is essential for photoreceptor ribbon synapse formation. Nat Neurosci 11, 923-931.

Shingai R, Hida E & Naka K. (1983). A comparison of spatio-temporal receptive fields of ganglion cells in the retinas of the tadpole and adult frog. Vision Res 23, 943-950.

Sterling P & Matthews G. (2005). Structure and function of ribbon synapses. Trends Neurosci 28, 20-29.

Tian N & Copenhagen DR. (2001). Visual deprivation alters development of synaptic function in inner retina after eye opening. Neuron 32, 439-449.

tom Dieck S & Brandstatter JH. (2006). Ribbon synapses of the retina. Cell Tissue Res 326, 339-346.

Tootle JS. (1993). Early postnatal development of visual function in ganglion cells of the cat retina. J Neurophysiol 69, 1645-1660.

Wassle H. (2004). Parallel processing in the mammalian retina. Nat Rev Neurosci 5, 747-757.

Wong RO. (1990). Differential growth and remodelling of ganglion cell dendrites in the postnatal rabbit retina. J Comp Neurol 294, 109-132.

Wong RO & Godinho L. (2003). Development of the Vertebrate Retina. In The visual neurosciences, ed. Chalupa LM & Werner JS, pp. 77. The MIT Press.

6. Table

Table 1. Correlation coefficients of spatial STA values and dendrite densities

ON						OFF					
P10-14		P20-23		Adult		P10-14		P20-23		Adult	
R	p	R	p	R	p	R	p	R	p	R	p
0.396	0.033	0.767	0.01	0.525	0.065	-0.412	0.184	-0.497	0.026	-0.504	0.005
0.409	0.048					-0.544	0.005	-0.590	0.000	-0.217	0.096
0.518	0.000					-0.381	0.080	-0.150	0.350	-0.356	0.033
						-0.120	0.695				
						-0.406	0.019				

R is the Pearson's correlation coefficient. Each pair of R and p-value was from one alpha cell at different development stages. The p-values are for testing the hypothesis of no correlation.

7. Figures

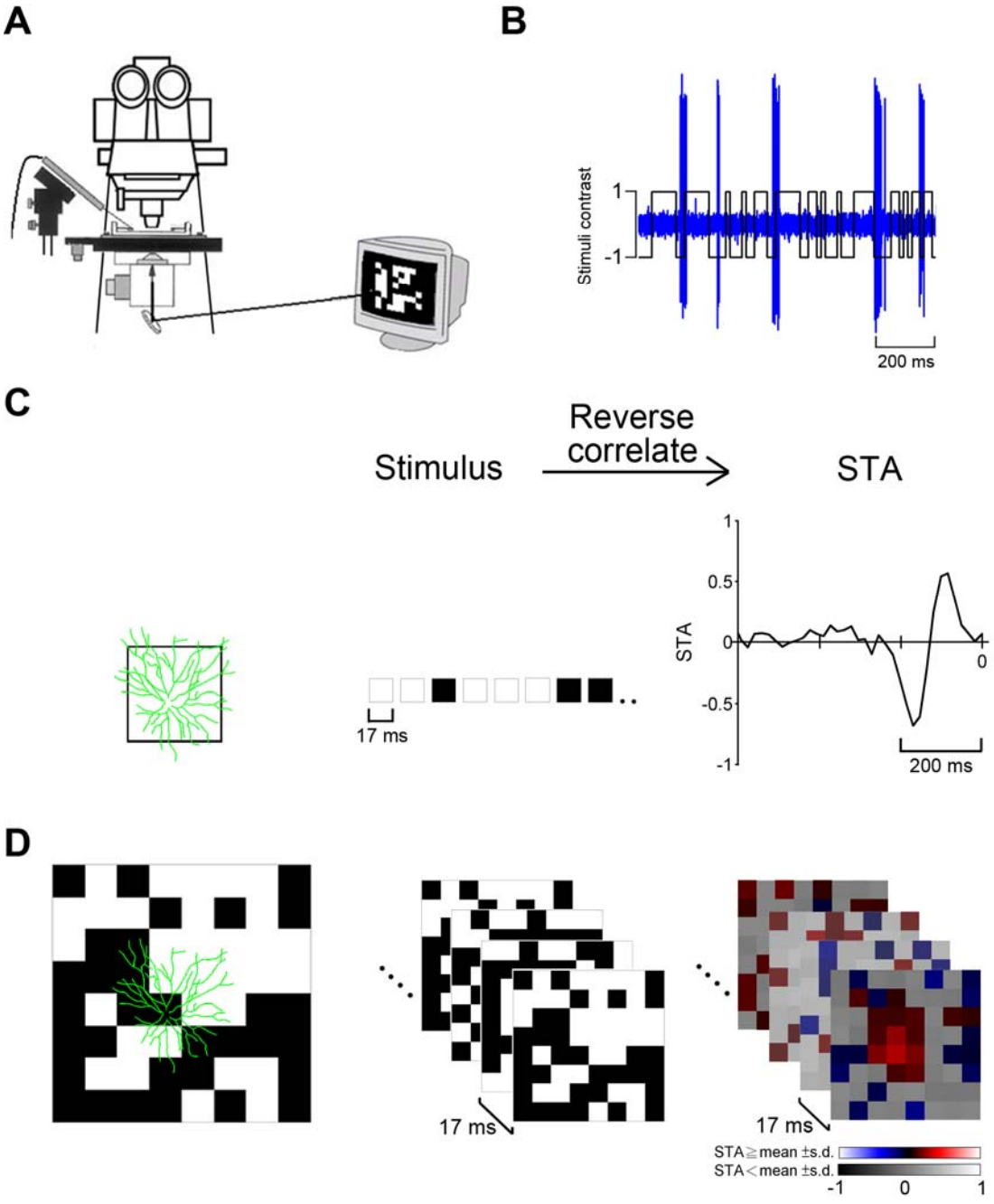

Figure 1. Diagram of experimental setup and the visual stimulus used.

(A) Visual stimuli were displayed by a CRT monitor and reflected upward by a mirror beneath the microscope stage. A 20× microscope objective replaced the condenser of

microscope was used to focus the stimulus onto the photoreceptor layer of the retina. The black line represents the path of light. Neural response of alpha RGC was recorded by tungsten-in-glass electrode. (B) A demonstration of spikes (blue plot) that recorded while the RGC was given white noise stimulation. Stepwise black stairs, 1 by 1white noise with only two colors, white and black, represented by 1 and -1. (C) Illustration of 1 by 1 white noise stimuli and corresponding result, the temporal profile of spike triggered average (STA). STA is calculated by reverse correlate the stimuli and response of cell. (D) 8 by 8 white noise stimuli and spatiotemporal STA results.

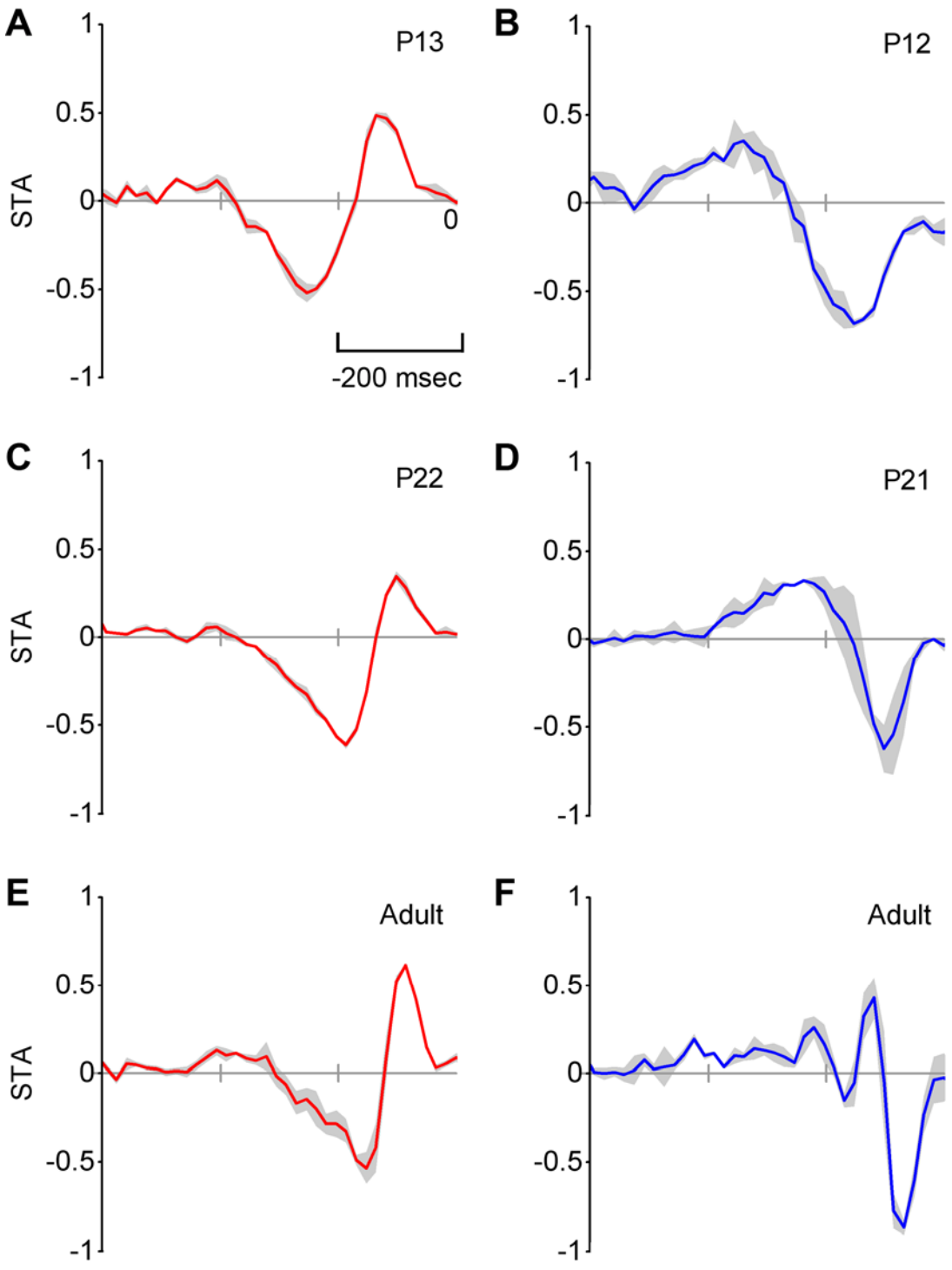

Figure 2. Temporal STA of ON and OFF alpha cells from different developmental stages.

(A)-(F) Temporal STA pattern from a single alpha RGC in each postnatal stage

P10-14, P20-23, and adult to exemplify the physiological change of alpha RGCs during development. The results came from 3 to 4 trials of temporal varying white noise stimuli centered on receptive field of alpha RGCs. STA, mean ± s.d. (shadow). STA is an averaged stimulus intensity function that alters along a time course before a spike, which occurs at time point zero. Red, ON alpha cell; blue, OFF alpha cell.

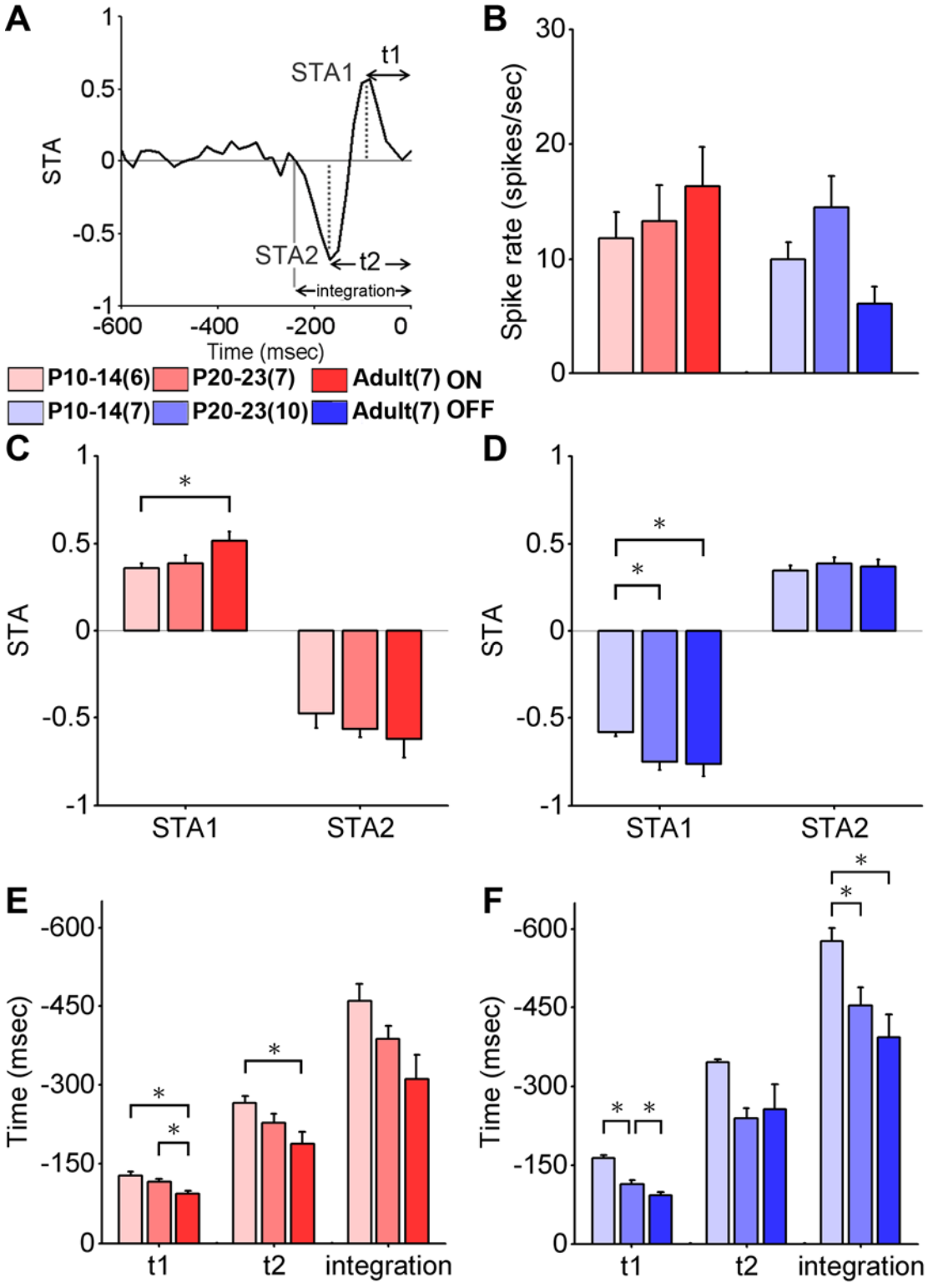

Figure 3. Characteristics of temporal STA of ON and OFF alpha cells change during development, indicating that physiological function of ON and OFF RGCs still develop after eye-opening at P10.

(A) The characteristic parameters of temporal STA were from populations of ON and OFF alpha RGCs at postnatal stage P10-14, P20-23, and adult. Representative colors for each group are as annotated, and the sample sizes are in the parentheses. Inset is a temporal STA profile of single RGC as in Fig2, the parameters are as designated in the illustration. STA1 is the first peak STA value near the zero time point, and STA2 is from the second peak value with inverse sign. Three indexed time points were taken to analysis, time to the first peak (t1), time to the second peak (t2), and the zero-crossing point of STA profile after the second peak, also known as integration time. Each parameter is expressed as mean ± s.e.m. in (C) - (F). * indicates statistical significance of different development stages comparisons and *p*-value is < 0.05. (B) Spike rate were total recorded spikes divided by time lapse of given white noise stimuli. Spike rate had a little tendency of increase in ON alpha cells during development. STA1 and STA2 of (C) ON alpha cells, and (D) OFF alpha cells. Indexed time points of (E) ON alpha cells, and (F) OFF alpha cells.

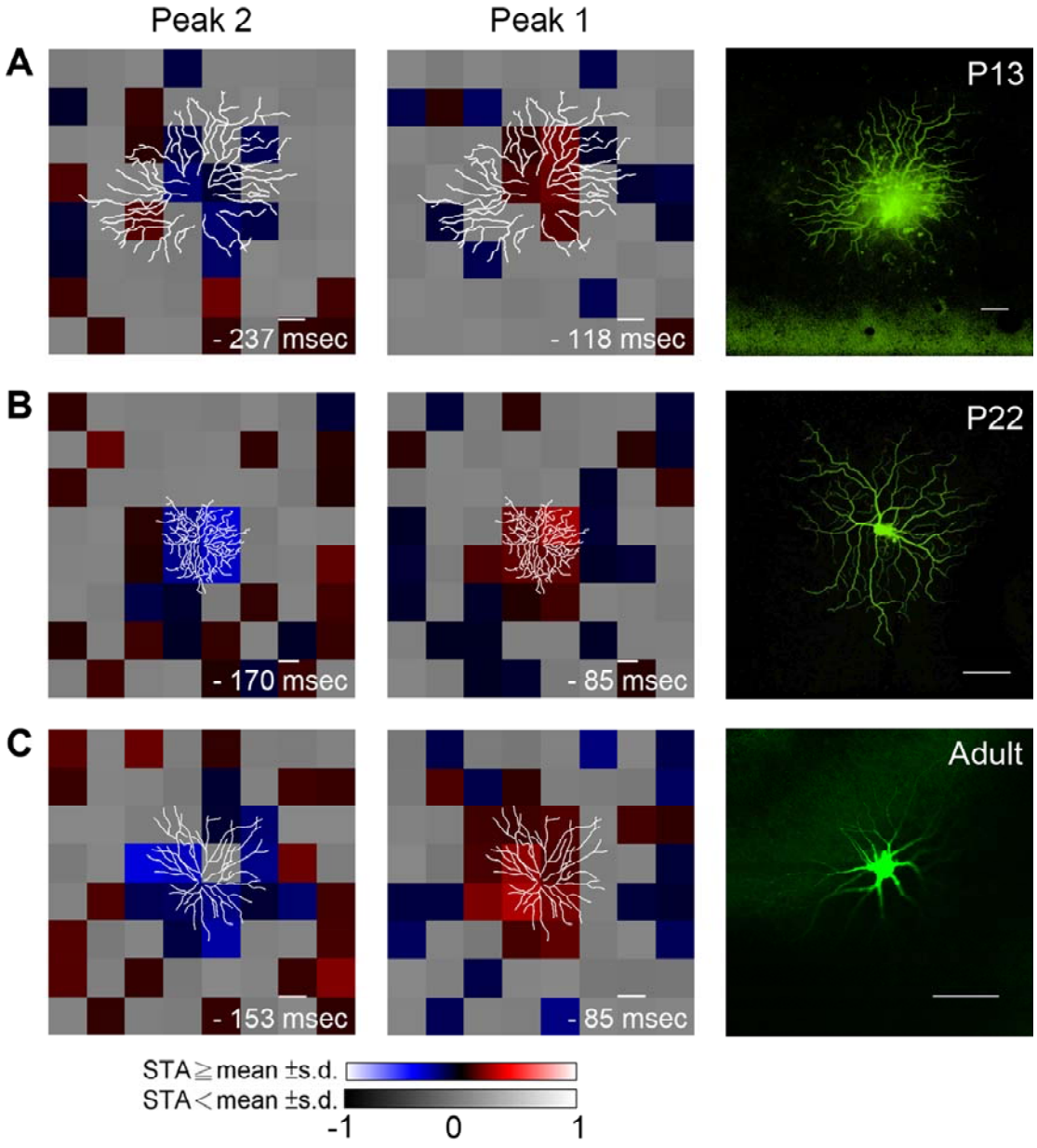

Figure 4. Spatiotemporal STA of ON and OFF alpha cells alter at different developmental stages.

(A) - (C) ON alpha cells effective spatiotemporal STA profiles at time of peak 1 and peak 2, which are juxtaposed with morphology of the corresponding cells. Camera lucida of the RGC dendritic pattern (white drawings) was oriented to align with the given 8 by 8 white noise stimuli, ant it was also rescaled according to the width of

white noise stimuli. Colorbar, color scale represents STA value from -1 to 1. While STA values exceeding one standard deviation (s.d.) in each frame, the exact pixels would be color coded to demonstrate their magnitude. The red pixels represent that RGC was excited by intensity increase, or inhibited by intensity decrease at those locations. The blue ones were on the contrary excited by intensity decrease, or inhibited by intensity increase. Gray scale bar, gray scale for STA value from -1 to 1 at the pixels with values close to mean (zero) within one s.d.. Scale bar, 100 μm.

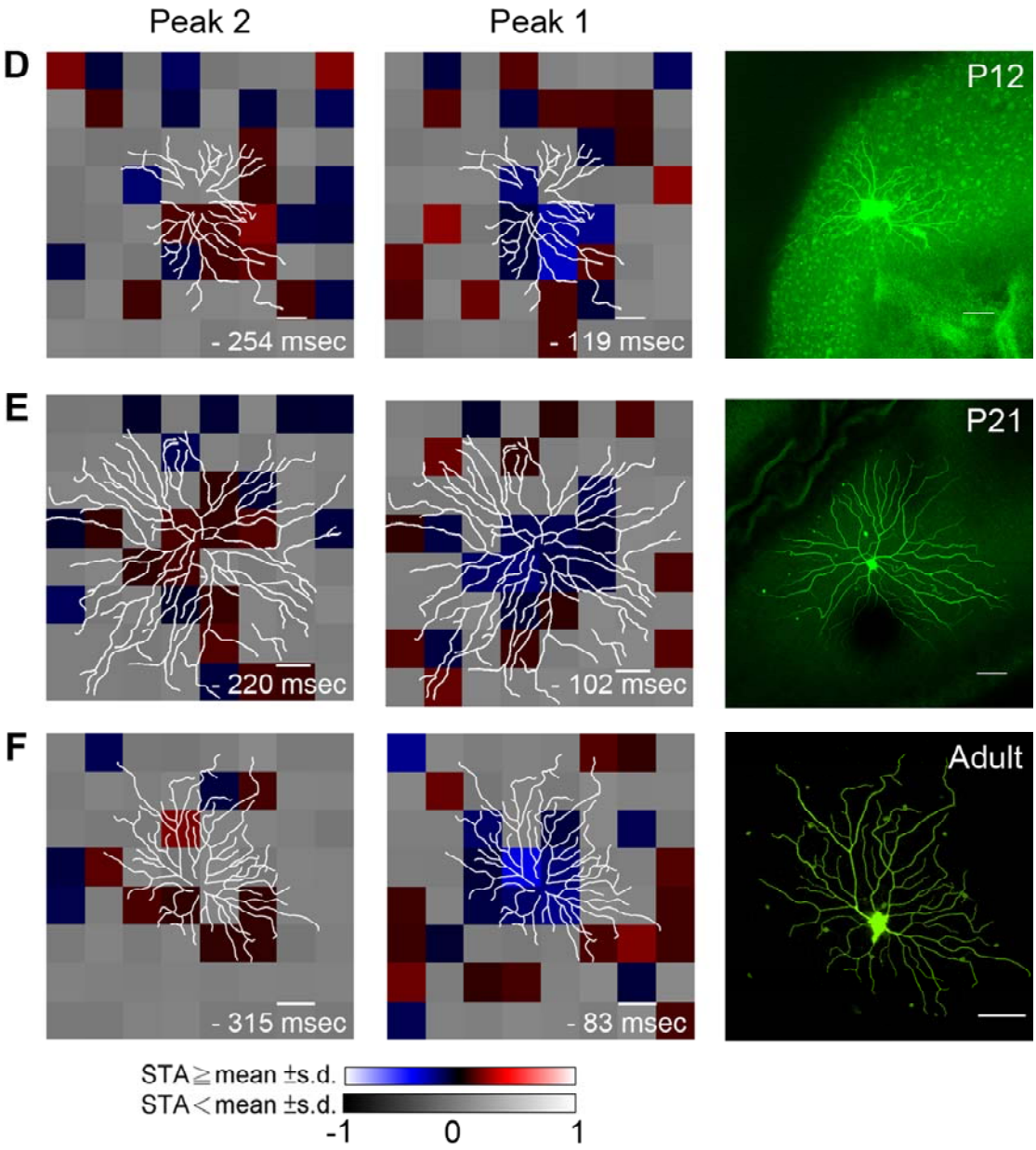

Figure 4. Spatiotemporal STA of ON and OFF alpha cells alter at different developmental stages. (continued)

(D) - (F) OFF alpha cells effective spatiotemporal STA profiles at time of peak 1 and peak 2. Time of peak 1 and peak 2 in serial spatiotemporal STA frames were decided by the procedure described in methods and Appendix 2.

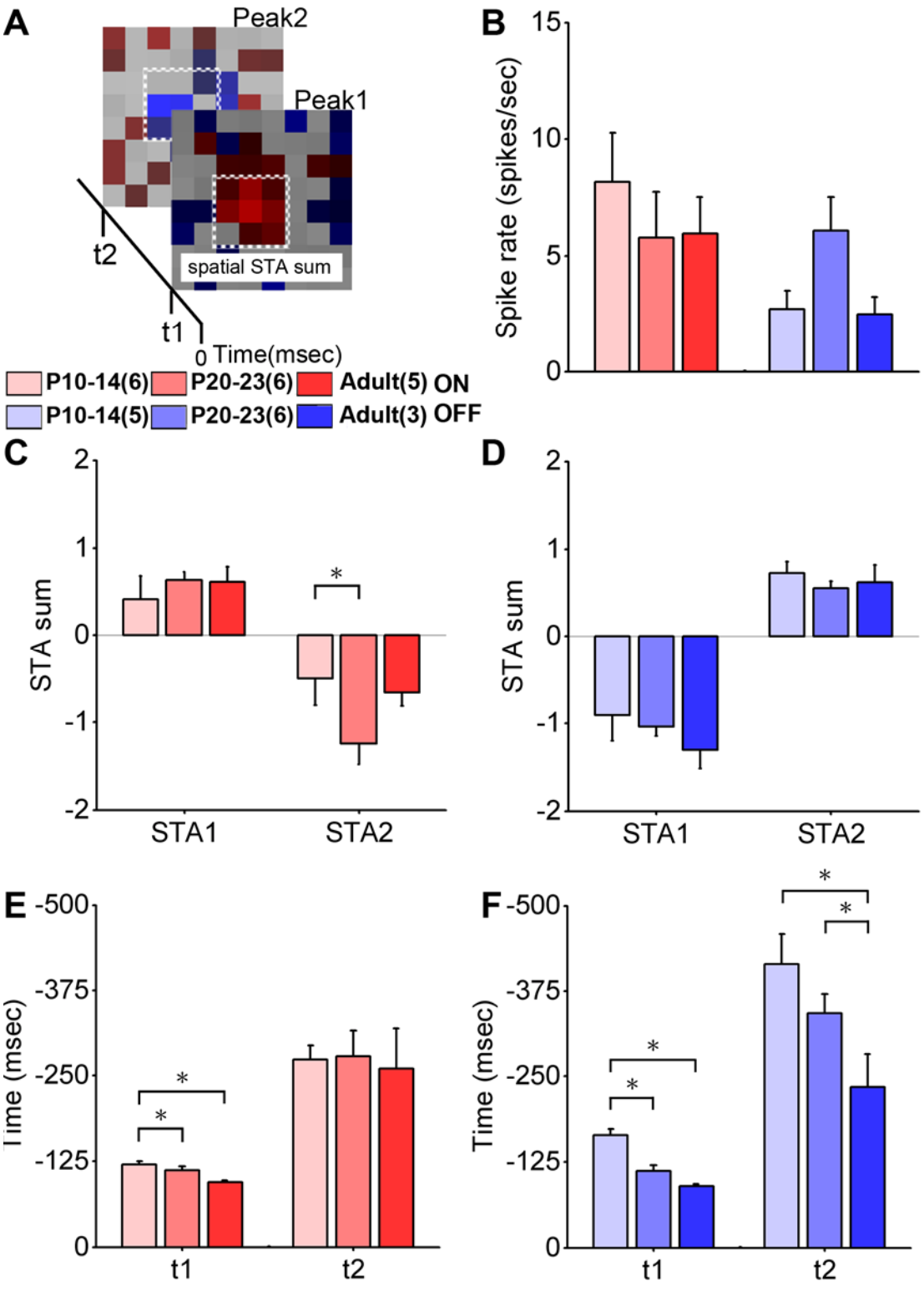

Figure 5. Characteristics of spatiotemporal STA of ON and OFF alpha cells alter during development.

(A) Parameters of effective STA profiles were examined. T1 and t2 are the respective

time of frame at peak 1 and peak 2. Spatial STA sum is the cumulation of STA values pixel by pixel around the pixel with largest absolute STA, which would also be included, so there are nine counted pixels in total as contoured by dot line on the STA profile. Representative colors for each group are as annotated, and the numbers of cells in particular populations are in the parentheses. * indicates statistical significance of different development stages comparisons and *p*-value is < 0.05. (B) Spike rate were total recorded spikes divided by time lapse of given 8 by 8 white noise stimuli. STA sum at peak 1 (abbreviated ad STA1) and peak 2 (STA 2) of (C) ON alpha cells, and (D) OFF alpha cells. Tl an t2 of (E) ON alpha cells, and (F) OFF alpha cells.

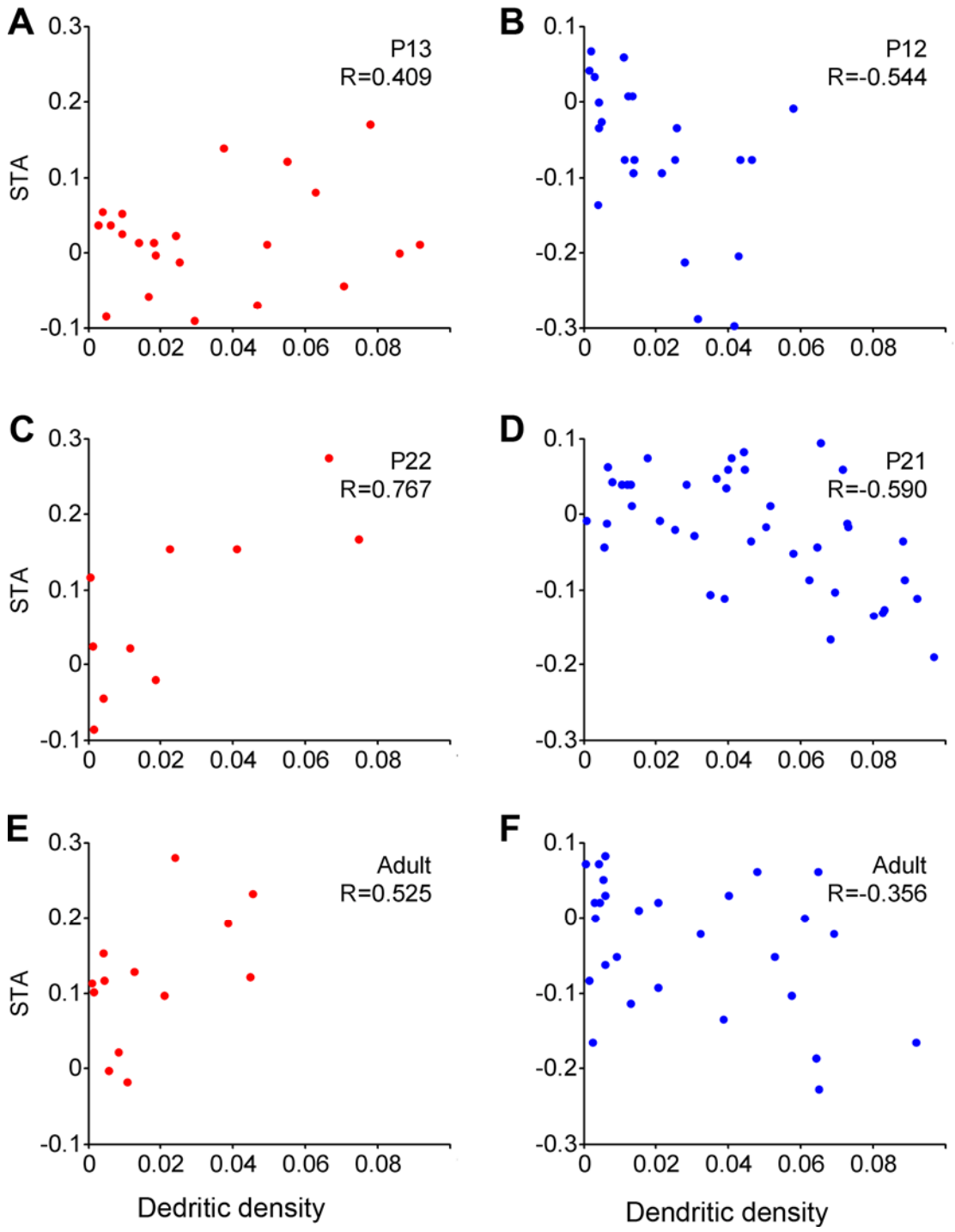

Figure 6. Correlation between spatial STA values and dendritic densities of developing ON and OFF alpha cells.

(A) - (F) Scatter plot of STA values versus dendritic densities from a single alpha RGC at postnatal stage P10-14, P20-23, and adult to demonstrate the correlation in

between. STA values are the values of effective STA profile at tl. R, Pearson's correlation coefficient. Red, ON alpha cells; blue, OFF alpha cells.

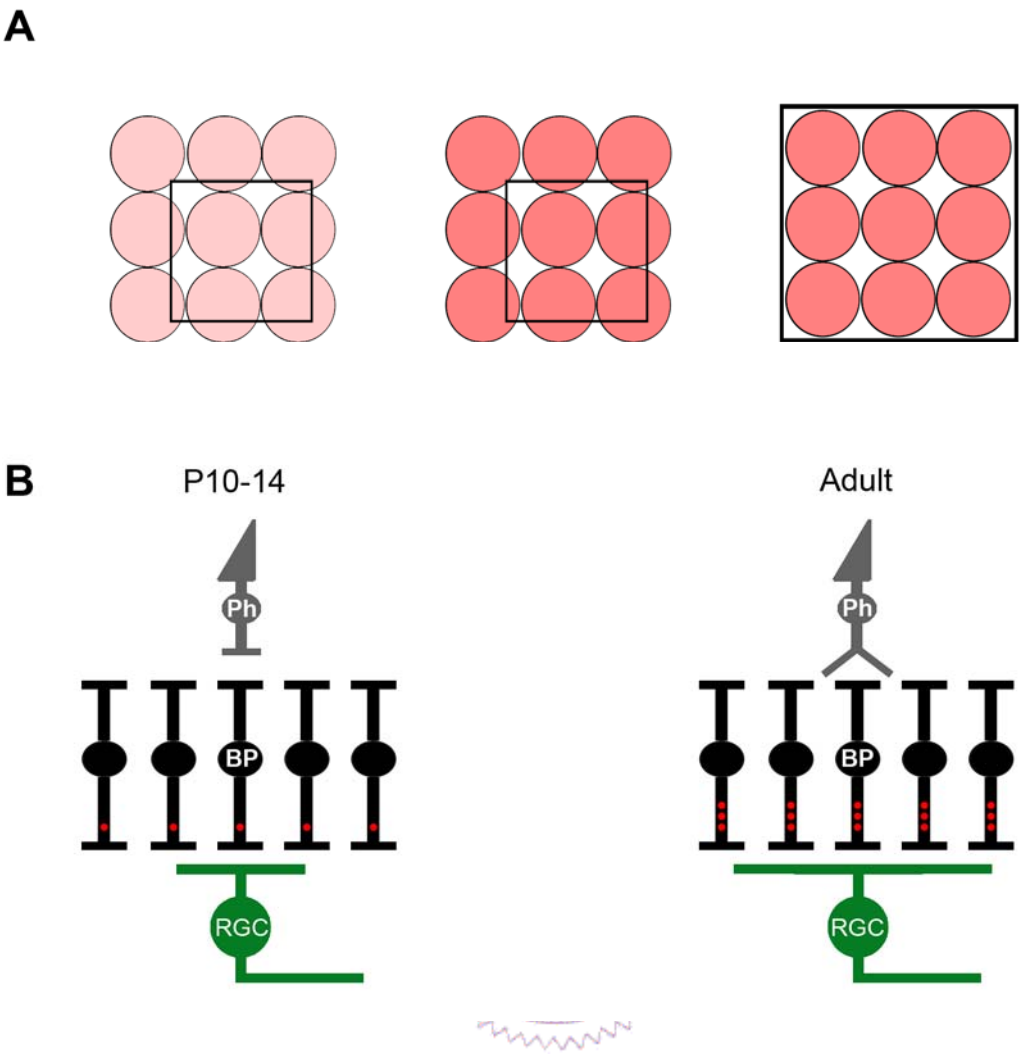

Figure 7. Model for functional maturation of alpha RGC during development.

(A) Black frameworks of squares represent the approximate extent that RGC could receive input from upstream neurons. At left, immature has a smaller dendritic arbor thus they may gather neural input in a smaller region. Further, the light red circles represent one arbitrary unit of excitatory input, which are composed by bipolar cells. Light color stands for weaker input while comparing to the red circle at middle and right. Middle is a predicted situation deduced from our results that one adult ON alpha cell had relative small dendrite arbor that similar to alpha cell at stage P10-14 (Fig 4A

and 4C). However, it is found that there are more pixels with high STA values within the extent of the adult RGC's dendritic filed than the P10-14 alpha cell. The widths of one pixel in STA profiles from these two cells are also similar. Thus, it seems to be that the spatial array of excitatory input unit are unchanged, and it is the increase of input strengths or activities instead. Considering that a matured alpha cell usually has a quite large dendritic arbor (as depiction at right), both the numbers of input units and the strength of each unit might both increase during development. (B) Potential mechanisms that affect spatiotemporal receptive field maturation of alpha RGC after eye-opening in the rabbit retina. From P10-14 to Adult, the contact pattern between photoreceptor cells (Ph, gray) and bipolar cells (Bp, black) represents structural maturation of ribbon synapses (from a horizontal line to a fork branch). Similarly, the increased numbers of red dots at the axonal terminals of bipolar cells, next to ganglion cells (RGC, green), indicate synaptic maturation of ribbon synapses. These structural and synaptic changes might contribute to our observations in this study (see discussion). As described above, the fact that the alpha ganglion cell increased the dendritic arbor from P10-14 to Adult correlates with the notion that the functional maturation of alpha RGCs might be attributed to the increased strength of synaptic input, and/or total number of connecting bipolar cells, rather than the alteration of the existing bipolar cell array.

8. Appendixes

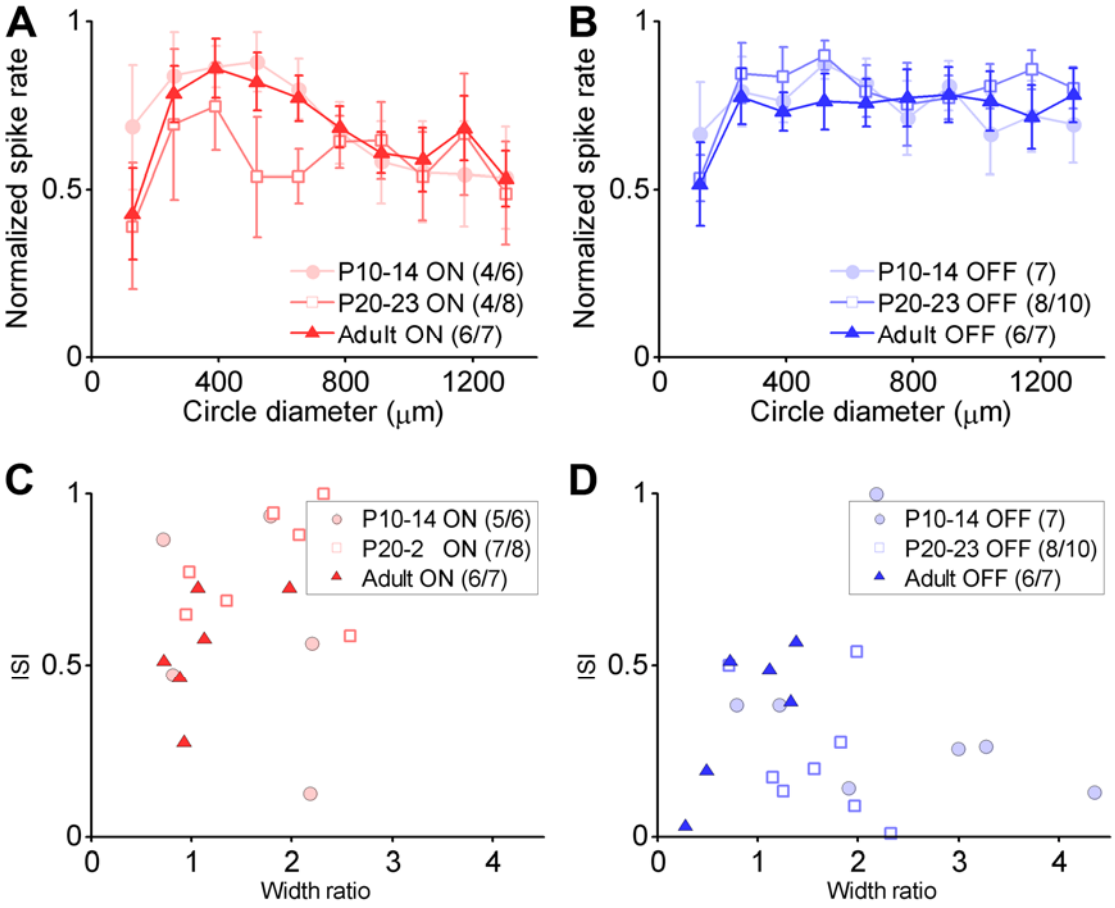

Appendix 1. The classical center-surround organization of receptive fields in ON and OFF alpha RGCs at different development stages were not different after eye-opening of the rabbits.

Classical receptive field properties of (A) ON alpha and (B) OFF alpha cells were detected by a flashing (167 ms) white circle with increasing diameters (the circle test). Normalized response of alpha cells to differ circle diameters (mean ± s.e.m.) from age

groups P10-14 (closed circle), P20-23 (open square), and adult (closed triangle). The numbers of cells are in parentheses. (C)-(D) The width ratio is the ratio of the width of one by one white noise stimuli to the interpolating diameters with strongest center-along response in the circle test of each cell. The scatter plots are inhibition strength index (ISI) versus the width ratio of cells from the three age groups with same symbols as above. The numbers of partial cells that had been tested their ISI in particular developmental stages are in the parentheses.

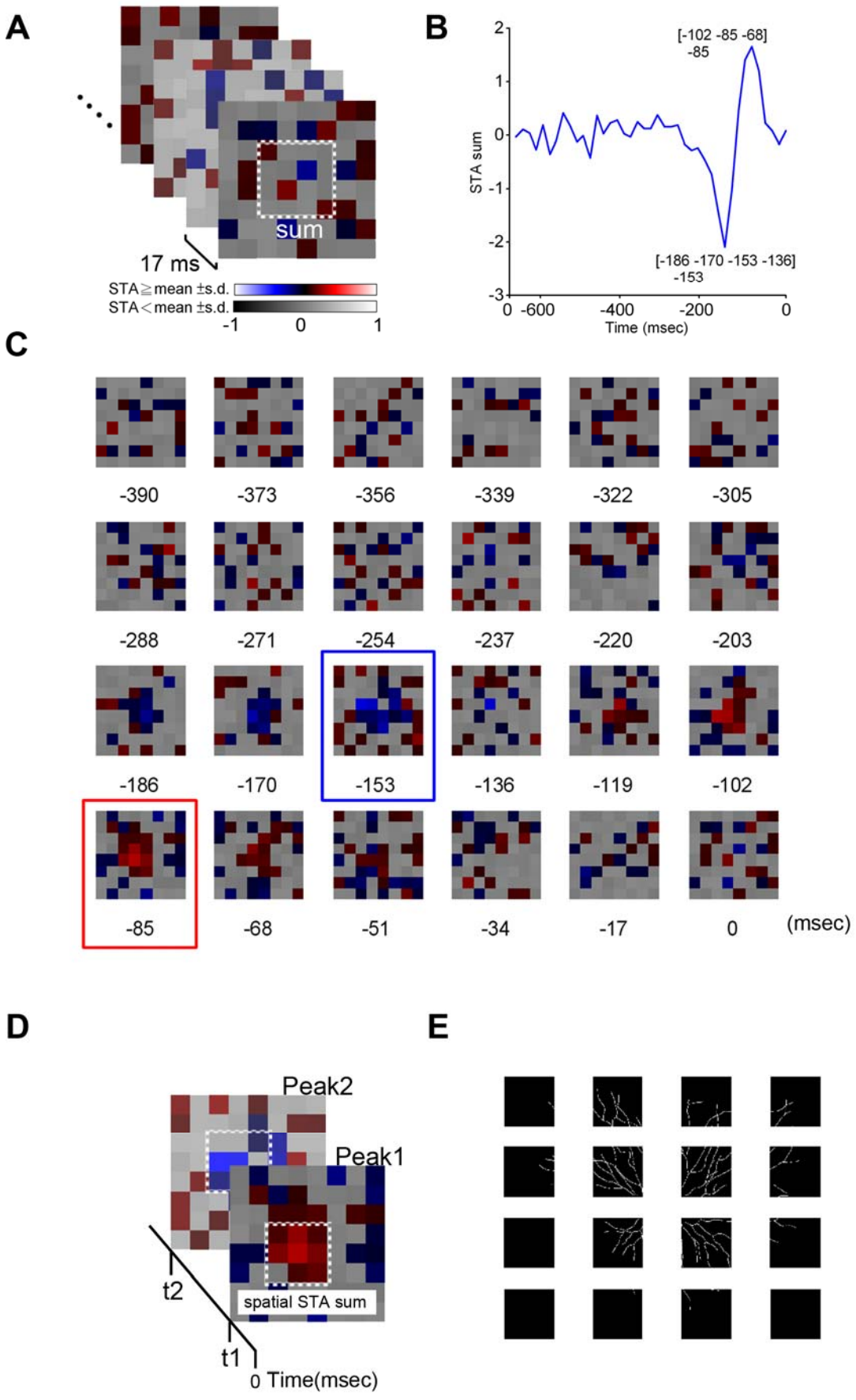
A
sum
17 ms
STA≧mean ±s.d.
STA＜mean ±s.d.
-1
0
1
B
[-102 -85 -68]
-85
[-186 -170 -153 -136]
-153
STA sum
Time (msec)
C
-390
-373
-356
-339
-322
-305
-288
-271
-254
-237
-220
-203
-186
-170
-153
-136
-119
-102
-85
-68
-51
-34
-17
0
(msec)
D
Peak2
Peak1
t2
t1
spatial STA sum
0 Time(msec)
E

Appendix 2. The methods of defining the effective frames in whole series of spatiotemporal STA results, and the calculation of dendritic densities of RGC.

(A) The result of each 8 by 8 white noise stimulus trial is a series of frames, the spatial STA profiles before spike at time point zero. To find out the effective STA profiles that could represent high sensitivities in the receptive field of one alpha RGC. In each single STA frame, the STA values of central 4 by 4 pixels were summed up. (B) The values of central STA sum from each frame come into a function (blue plot) of time. The time point at maximum and minimum of this function is defined as t1 (e.g. -85ms in result of this trial) and t2 (e.g. -153ms). In addition, it had been checked that the peak value would be accompanied with other values (as annotated in brackets) large than one standard deviation of all the STA sums. Thus, the peaks of STA sum would not be and randomly appear ones. (C) The corresponding effective STA profiles at t1 (-85ms, circumscribed by red contour) and t2 (-153ms, blue contoured one) in this example. (D) Effective STA profiles at t1 and t2 are for successive parameters analysis, the population results are in Fig. 5. (E) In order to compare the morphological and physiological properties of alpha RGCs during development, the camera lucida of dendritic pattern (the white arbor) of a alpha cell would be divided to calculate the dendritic density. The width of each division is as same as the width of one pixel in the 8 by 8 white noise stimulus that used to stimulate the cell.

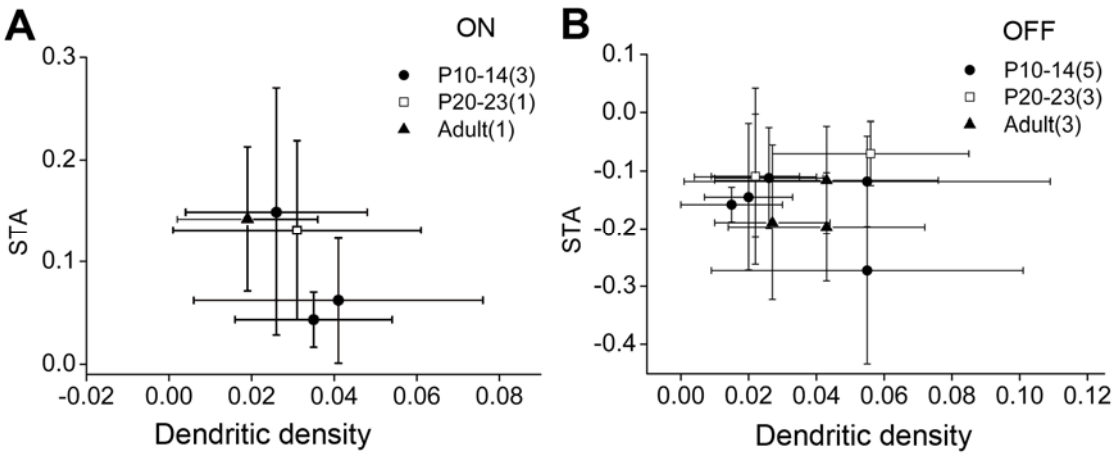

Appendix 3. Distribution of dendritic densities and STA values of each ON and OFF alpha cells at different development stages.

(A) At different development stages, in each ON alpha cell, results of dendritic densities and STA values in effective STA profile at tl are plotted as mean±s.d to demonstrate their variation. Closed circle, P10-14; open square, P20-22; closed triangle, adult; numbers of cells are in the parentheses. (B) Relative results in OFF alpha cells.